IOPscience iopscience.iop.org

Home Search Collections Journals About Contact us My IOPscience

Interfacial and defect structures in multilayered GaN/AlN films

This article has been downloaded from IOPscience. Please scroll down to see the full text article.

2002 J. Phys.: Condens. Matter 14 13277

(http://iopscience.iop.org/0953-8984/14/48/378)

View the table of contents for this issue, or go to the journal homepage for more

Download details:
IP Address: 171.66.16.97
The article was downloaded on 18/05/2010 at 19:17

Please note that terms and conditions apply.

INSTITUTE OF PHYSICS PUBLISHING JOURNAL OF PHYSICS: CONDENSED MATTER

J. Phys.: Condens. Matter **14** (2002) 13277–13283 PII: S0953-8984(02)53989-8

Interfacial and defect structures in multilayered GaN/AlN films

Ph Komninou[1,4], Th Kehagias[1], J Kioseoglou[1], G P Dimitrakopulos[1], A Sampath[2], T D Moustakas[2], G Nouet[3] and Th Karakostas[1]

[1] Department of Physics, Aristotle University of Thessaloniki, 541 24 Thessaloniki, Greece
[2] Electrical and Computer Engineering Department, Physics Department and Center for Photonics Research, Boston University, Boston, MA 02215, USA
[3] ESCTM-CRISMAT, UMR 6508 CNRS, ISMRA, 6 Boul. Marechal Juin, 14050 Caen Cedex, France

E-mail: komnhnoy@auth.gr

Received 27 September 2002
Published 22 November 2002
Online at stacks.iop.org/JPhysCM/14/13277

Abstract
A structural assessment of various interfaces formed between successive GaN/AlN layers epitaxially grown on (0001) sapphire, as well as between n-type and p-type GaN is presented, using transmission and high-resolution electron microscopy. The structure of the interfaces between the thick GaN and the thin AlN interlayers (ILs) is investigated in terms of misfit difference and elastic fit of the two crystal lattices. Dense threading dislocations are observed to originate from the substrate/buffer layer interface and their interaction with the successive AlN ILs is studied. Furthermore, basal inversion domain boundaries localized in the n-GaN/p-GaN interface are evaluated.

1. Introduction

Gallium nitride is a material that has drawn a lot of attention in the last few years due to its potential applications in optoelectronic and microelectronic industries [1]. The fabrication of UV/blue-light-emitting diodes (LEDs) has been achieved by deposition of GaN, through various methods, on (0001) sapphire substrates. Since the misfit in lattice parameters of these two crystal lattices and the difference in their thermal expansion coefficients are appreciable, direct deposition of GaN on sapphire results in a three-dimensional growth of GaN islands at the early stages of growth. As a consequence, high densities of threading dislocations (TDs) are emerging from the interface. The growth of a buffer layer, usually AlN, between the substrate and the film to reduce the misfit does not appear to affect significantly the high dislocation density. Thus, GaN-based devices undergo a partial loss of their electronic transport properties.

In order to improve the crystalline structure of the GaN epilayers, several complex growth techniques have been applied. The use of epitaxial lateral overgrowth (ELO) in hydride vapour

[4] Author to whom any correspondence should be addressed.

phase epitaxy (HVPE) and metal–organic vapour phase epitaxy (MOCVD) appears to give the best results as regards the reduction of TD density and, thus, improving the efficiency of the device [1–5]. When using the molecular beam epitaxy (MBE) technique, growth of a single or multiple AlN interlayers (ILs) within the GaN epilayer is used for the same purpose. High-temperature-grown AlN ILs seem to reduce dislocation densities to the subsequent GaN layers, by forcing TDs to interact and annihilate or to bend within the AlN ILs [2–6]. The decrease ratio of TDs, however, appears to be associated with several inherent variables, namely the thickness of the IL, the TD character, the distance between successive AlN IL, as well as the polarity of the GaN epilayer [2–8]. Conversely, observations on GaN films with low-temperature-grown AlN ILs gave controversial results concerning the reduction or the multiplication of TDs [7–9].

In this work, a structural assessment of various interfaces formed between successive GaN/AlN layers grown by MBE on (0001) sapphire at high temperature, as well as between n-type and p-type GaN is presented, using conventional and high-resolution transmission electron microscopy (TEM–HRTEM). The interfacial structure between the thick GaN and the thin (of the order of a few lattice spacings) AlN IL is investigated in terms of misfit difference and elastic fit of the two crystal lattices. TDs are observed to originate from the substrate/buffer layer interface and their interaction with the successive AlN ILs is studied. Furthermore, basal inversion domain boundaries (IDBs) on the n-GaN/p-GaN interface are evaluated.

2. Experimental details

The GaN film investigated was grown by plasma-assisted MBE on (0001) sapphire with a 25 nm thick AlN buffer layer and two thin AlN ILs separated by two 100 nm thick n-GaN spacer layers. The entire multilayer film was grown at a temperature of 750 °C following the scheme: substrate Al_2O_3; 25 nm AlN; 100 nm n-GaN; 3 nm AlN; 100 nm n-GaN; 3 nm AlN; 3 μm n-GaN; 0.5 μm p-GaN. As described, up to the top 3 μm of the GaN layer the film was n-type Si doped, while in the last 0.5 μm of GaN growth the flux of dopant changed from Si to Mg and the layer was p-type doped. All layers were grown under group-III-rich conditions of growth, which generally leads to films with smooth surfaces. Evidence for the polarity of the film was provided *in situ* by reflection high-energy electron diffraction (RHEED), while the polarity of the surface of the top layer was found upon etching of the sample in a KOH-based solution heated to 80 °C for 2 min. Moreover, the polarities of the n-GaN and p-GaN layers were verified by convergent beam electron diffraction (CBED).

Samples for TEM–HRTEM observations were cut in cross-section orientation and thinned to transparency by the standard procedure of mechanical grinding followed by appropriate Ar-ion milling. TEM observations were carried out in a Jeol 120CX electron microscope operated at 100 kV, whereas HRTEM and CBED observations were performed in a Jeol 2010 electron microscope operated at 200 kV, with a point resolution of 0.19 nm and $C_s = 0.5$ mm.

3. Results

Three types of TD were, generally, present in the sample: type $\boldsymbol{a}$ with $\boldsymbol{b} = (1/3)\langle 11\bar{2}0\rangle$, type $\boldsymbol{a}+\boldsymbol{c}$ with $\boldsymbol{b} = (1/3)\langle 11\bar{2}3\rangle$ and type $\boldsymbol{c}$ with $\boldsymbol{b} = \langle 0001\rangle$. The TD densities found are given in table 1. As is evident, the $\boldsymbol{c}$-type dislocations are gradually reduced from the buffer layer to the surface by 45%, whereas dislocations of $\boldsymbol{a}$ and $\boldsymbol{a}+\boldsymbol{c}$ type are reduced by only by 5%. Figure 1 illustrates two weak-beam (WB) ($\boldsymbol{g}/3\boldsymbol{g}$) TEM micrographs of the same area taken with the 0002 and $10\bar{1}0$ reflections, respectively. Dislocations that are present in both micrographs are characterized as $\boldsymbol{a}+\boldsymbol{c}$ type, while ones of type $\boldsymbol{c}$ appear only in figure 1(a) and ones of type $\boldsymbol{a}$ only in figure 1(b).

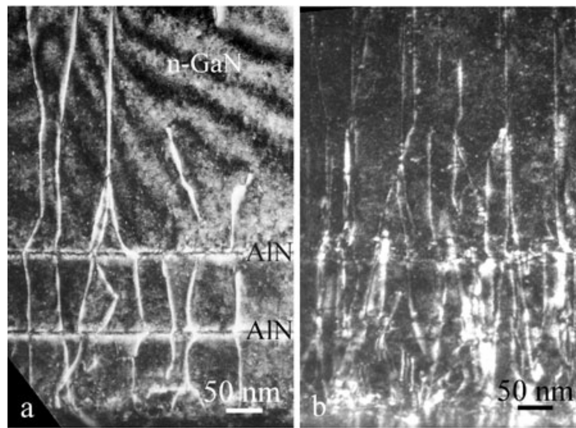

Figure 1. WB ($g/3g$) cross-section TEM micrographs showing the same area of the sample: (a) with $g = 0002$ where the c-component of the TDs is visible; (b) with $g = 10\bar{1}0$ where TDs with an a-component are in contrast.

Table 1. Densities of the different types of TD in the successive GaN layers.

	Type a (10^{10} cm^{-2})	Type $a + c$ (10^{10} cm^{-2})	Type c (10^{9} cm^{-2})
1st spacer (n-GaN)	7.2	2.1	2.2
2nd spacer (n-GaN)	7.2	2.1	2.0
Overlayer (n-GaN)	6.8	2.0	1.5

The HRTEM image of figure 2 illustrates the structure of the successive GaN/AlN IL/GaN interfaces viewed along the $[11\bar{2}0]$ zone axis. Due to the natural lattice mismatch between GaN and AlN, the in-plane misfit is almost 2.5%. Fourier filtering in a series of such HRTEM images from both AlN ILs, using only the in-plane spatial frequencies, revealed a pseudomorphic growth of the ILs on GaN spacer layers, where no regular array of misfit dislocations was detected. Since the AlN ILs are strained, interaction of TDs with the ILs is expected to occur (figure 2). Our observations showed the following.

(a) When crossing the GaN/AlN interfaces, the existing strain field forces the TDs to change their line direction. If there is an adequately thick GaN layer over the AlN IL, then the conditions for dislocation interactions will be favourable. In the case of c-type dislocations, annihilation can occur when two opposite Burgers vectors meet. Moreover, c-type dislocations tend to form half-loops with increasing GaN epilayer thickness and fail to reach the surface (figure 3(a)) [10].

(b) When the strain interfacial energy is large enough, bending of TDs onto the basal plane occurs. Consequently, dislocations with an a-type Burgers vector component become screw and they can either continue to glide on their slip plane, restoring their initial line direction, or cross-slip to a 60° orientation creating, locally, a finite length of misfit dislocation lines [11]. After the formation of misfit segments, TDs continue to propagate towards the surface on a parallel prismatic slip plane. These dislocations, on reaching the upper interface of the IL, can either cross it or bend again onto the basal plane, leaving misfit segments in that interface as well (figure 2). Thus, half-loops are formed within the AlN IL (figures 3(b), (c)).

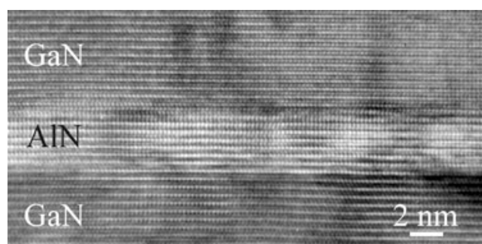

Figure 2. A HRTEM image illustrating the structure of the successive GaN/AlN IL/GaN interfaces viewed along the [11$\bar{2}$0] zone axis. TDs that change their line direction when crossing the GaN/AlN IL interfaces or bend onto the basal plane are visible.

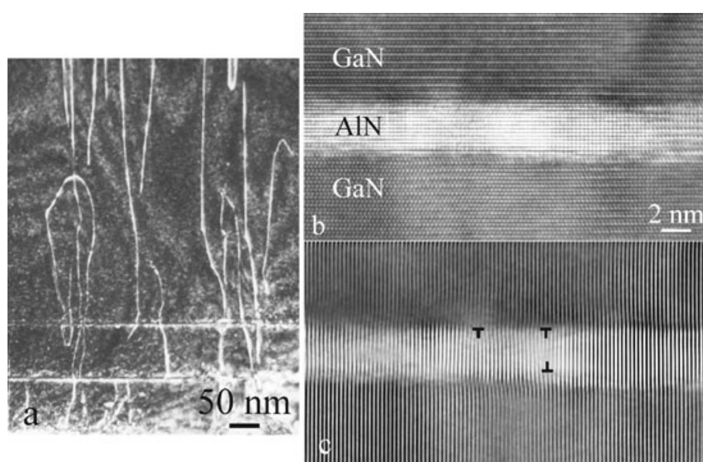

Figure 3. (a) A WB ($g/5g$) cross-section TEM micrograph showing c-type TDs forming half-loops with increasing GaN epilayer thickness. (b) A HRTEM image, viewed along the [11$\bar{2}$0] zone axis, illustrating the bending of TDs onto the successive GaN/AlN IL/GaN interfaces, while they continue to propagate towards the surface. (c) A Fourier filtered image of (b), where extra AlN IL half-planes are depicted, revealing the local appearance of misfit dislocation segments in the interfaces. The two opposite misfit segments in the same {10$\bar{1}$0} plane indicate the position of a half-loop.

We have evidence that, during the growth of the sample, the film up to the topmost n-type layer is of Ga polarity. This was derived from the 2×2 surface reconstruction observed *in situ* by RHEED [12]. However, after the deposition of the p-GaN layer, no reconstruction was evident either at the growth temperature or upon cooling. Nevertheless, we found that the p-type layer was N polar, based upon etching of the sample in a KOH-based solution heated to 80 °C for 2 min. CBED patterns taken from both sides of the same area of the p–n interface, combined with simulated CBED patterns, revealed the Ga polarity of the n-GaN layers while p-GaN is N polar. We shall show that the polarity change is related to Mg doping.

During the growth of p-GaN with a high Mg flux, the incorporation of a high concentration of Mg should cause clustering of Mg atoms or incorporation in interstitial or lattice sites. Experimental observations showed the formation of planar and/or pyramidal defects [13–16]. It has also been suggested that Mg clustering may lead to the formation of Mg_3N_2 precipitates [17, 18]. As shown in figure 4(a), IDBs on {10$\bar{1}$0} prismatic planes emanate from the p–n interface, which contains cubic islands a few atomic layers thick, presenting an image

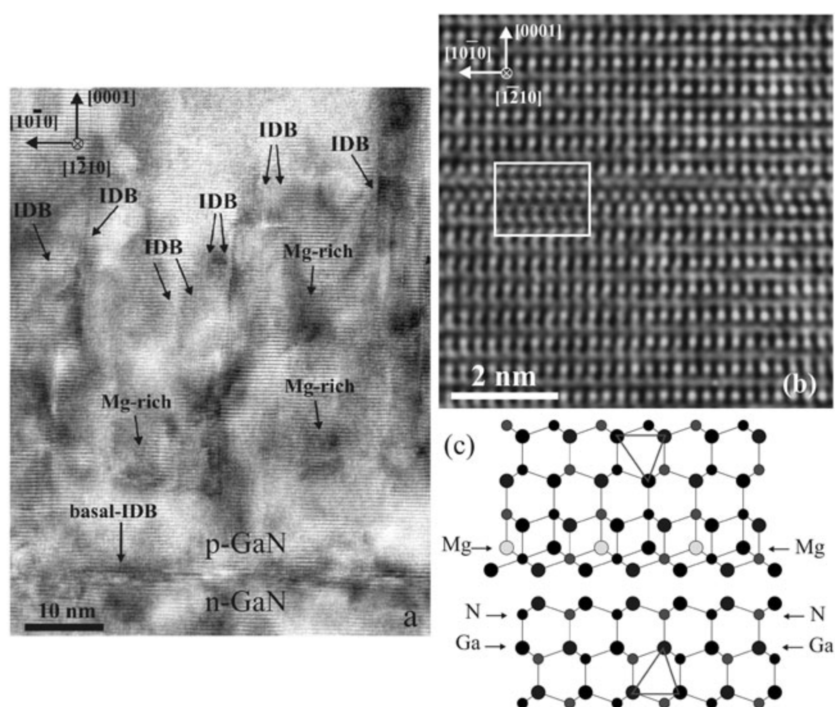

Figure 4. (a) A HRTEM micrograph showing the p-GaN epilayer containing prismatic IDBs that emanate from the p–n interface and Mg-rich clusters. (b) A HRTEM image from a part of the p–n interface; cubic Mg-rich islands identified as basal IDBs are confined at the p–n interface, leading the dominant polarity of the p-type region to be inverted with respect to that of the n-type region. The corresponding simulated image is given as an inset (thickness 3.2 nm, defocus −66 nm). (c) The supercell employed for HRTEM image calculations.

similar to that of a stacking fault (SF). The cubic islands cover extended areas of the p–n interface, terminating in sessile dislocations and bounded by prismatic IDBs. This leads to the conclusion that the dominant polarity of the p-type region is inverted with respect to the n-type region [19]. A similar state was observed in bulk GaN:Mg samples [13]. A part of the p–n interface is depicted in the HRTEM image of figure 4(b), where the SF-like structure is visible. Ramachandran *et al* [20] have proposed a model of a *c*-plane IDB comprising a local Mg_3N_2 structure. In order to investigate whether the observed configuration corresponds to such a bonding arrangement, we have undertaken image simulations. In figure 4(c) the supercell that was employed is given and the corresponding simulated image is shown as an inset in figure 4(b). The simulation gives satisfactory correspondence with the experimental image, indicating that the Ramachandran *et al* model is in agreement with our observations.

Other Mg extended defects in the form of regular or truncated pyramids were also observed, indicated as Mg-rich areas in figure 4(a), but they are not analysed here.

4. Discussion

AlN ILs are introduced in order to reduce TD density and improve the crystalline structure of n- and p-GaN epilayers of the system under investigation. The small reduction of TDs with an edge component (see table 1) can be attributed to the following reasons.

(a) Although strained GaN/AlN interfaces affect the line direction of dislocations, the 100 nm thick GaN spacers do not allow numerous dislocation interactions. Therefore, thicker GaN spacers, of the order of at least 300 nm [2, 3], are required in order to increase dislocation interactions and reduce their density in the GaN overlayer.

(b) Small variations in thickness of the AlN ILs result in a local increase of the strain and, therefore, TDs are forced to bend onto the interface plane becoming screw dislocations or cross-slip to a 60° orientation forming misfit dislocation segments. After departing from the basal plane, their initial direction is restored even after half-loop formation within the IL, leaving misfit segments in both GaN/AlN interfaces. Thus, the prospect of TD interactions within the n-GaN overlayer is reduced.

The presence of misfit dislocation segments at the GaN/AlN interfaces indicates that, locally, the thickness of the AlN ILs exceeds the critical value for the formation of misfit dislocations. This explains the fact that in some areas of the ILs only a change of the line direction of TDs is observed, since the strain field is not high enough to bend dislocations onto the interface plane (below critical thickness). In other areas, where bending of dislocations as well as formation of half-loops occur, misfit segments associated with them show that the critical thickness is exceeded. It appears that in our growth conditions, the critical thickness of the AlN ILs is about 3 nm. Subsequently, high-temperature AlN ILs of such thickness cannot be considered as sources of new edge dislocations due to the lack of three-dimensional growth [12]. Moreover, the local appearance of misfit dislocations is connected only with pre-existing TDs, which can bend and cross-slip onto the GaN/AlN interface plane. Therefore, we suggest a pseudomorphic growth of the AlN ILs on n-GaN that is locally relaxed by irregularly spaced misfit dislocation segments.

The growth of N-polar p-GaN epilayer can be attributed to the formation of an ultrathin cubic layer within the p–n interface. This layer is produced by Mg clustering in the form of cubic Mg_3N_2 precipitates, and is accountable for the growth of p-GaN epilayer in an inverted orientation with respect to n-GaN. It has to be mentioned that the polarity reversal in the Mg-doped GaN layers is generally observed when films are grown at high Mg fluxes and the polarity reversal affects the doping efficiency [12].

Acknowledgment

This work was supported by the EU Project No HPRN-CT-1999-00040.

References

[1] Humphreys C, Karakostas Th and Ruterana P 2001 Interfaces and defects at atomic level *Phys. Status Solidi* b **227**

[2] Felder F, Stemmer J, Hauenstein R J, Rotter T, Sanchez A M, Ponce A, Molina S I, Mistele D, Klausing H, Semchinova O, Aderhold J and Graul J 2002 *Mater. Res. Soc. Symp. Proc.* vol 693, ed J E Northrup, J Neugebauer, S F Chichibu, D C Look and H Riechert (Pittsburgh, PA: Materials Research Society) p I3.34.1

[3] Sanchez A M, Pacheco F J, Molina S I, Stemmer J, Aderhold J and Graul J 2001 *Mater. Sci. Eng.* B **80** 299

[4] Kasukabe K, Kishino K, Kikuchi A, Yamada T, Sugihara D and Nakamura S 2001 *J. Cryst. Growth* **230** 387

[5] Kikuchi A, Yamada T, Nakamura S, Kasukabe K, Sugihara D and Kishino K 2001 *Mater. Sci. Eng.* B **82** 12

[6] Sanchez A M, Pacheco F J, Molina S I, Stemmer J, Aderhold J and Graul J 2001 *J. Electron. Mater.* **30** L17

[7] Iwaya M, Terao S, Hayashi N, Kashima T, Amano H and Akasaki I 2000 *Appl. Surf. Sci.* **159–160** 405

[8] Amano H and Akasaki I 2002 *Opt. Mater.* **19** 219

[9] Benamara M, Liliental-Weber Z, Mazur J H, Swider W and Washburn J 2000 *Mater. Res. Soc. Symp. Proc.* vol 595, ed R Feenstra, T Myers, M S Shur and H Amano (Pittsburgh, PA: Materials Research Society) p F99W5.8.1

[10] Rouviere J L, Arlery M, Daudin B, Feuillet G and Briot O 1997 *Mater. Sci. Eng.* B **50** 61
[11] Sugiura L 1997 *J. Appl. Phys.* **81** 1633
[12] Moustakas T D, Iliopoulos E, Sampath A V, Ng H M, Doppalapudi D, Mirsa M, Korakakis D and Singh R 2001 *J. Cryst. Growth* **227–228** 13
[13] Liliental-Weber Z, Benamara M, Washburn J, Grzegory I and Porowski S 1999 *Phys. Rev. Lett.* **83** 2370
[14] Vennegues P, Benaissa M, Beaumont B, Feltin E, De Mierry P, Dalmasso S, Leroux M and Gibart P 2000 *Appl. Phys. Lett.* **77** 880
[15] Benaissa M, Vennegues P, Beaumont B, Gibart P, Saikaly W and Charai A 2000 *Appl. Phys. Lett.* **77** 2115
[16] Liliental-Weber Z, Jasinski J, Benamara M, Grzegory I, Porowski S, Lambert D J H, Eiting C J and Dupuis R D 2001 *Phys. Status Solidi* b **228** 345
[17] Van de Walle C G, Stampfl C and Neugebauer J 1998 *J. Cryst. Growth* **189/190** 505
[18] Hansen M, Chen L F, Lim S H, DenBaars S P and Speck J S 2002 *Appl. Phys. Lett.* **80** 2469
[19] Romano L T, Northrup J E, Ptak A J and Myers T H 2000 *Appl. Phys. Lett.* **77** 2479
[20] Ramachandran V, Feenstra R M, Sarney W L, Salamanca-Riba L, Northrup J E, Romano L T and Greve D W 1999 *Appl. Phys. Lett.* **75** 808